

Available online at [www.sciencedirect.com](http://www.sciencedirect.com)

**jmr&t**  
Journal of Materials Research and Technology  
[www.jmrt.com.br](http://www.jmrt.com.br)



## Original Article

# Corrosion behavior of API 5L X65 steel subject to plastic deformation<sup>☆</sup>



Mariana Cristina de Oliveira<sup>\*</sup>, Rodrigo Monzon Figueredo, Heloisa Andréa Acciari, Eduardo Norberto Codaro

São Paulo State University, School of Engineering, Guaratinguetá, SP, Brazil

### ARTICLE INFO

#### Article history:

Received 20 November 2017

Accepted 23 February 2018

Available online 16 April 2018

#### Keywords:

API 5L X65

Plastic deformation

Corrosion

Electrochemical

### ABSTRACT

The API 5L X65 steel is widely used as one of the most economical and safe ways of transporting oil and gas. The significant number of accidents caused by failures of pipelines is due to corrosion. Plastic deformation can modify the mechanical properties of these pipelines, so study the steel's corrosive behavior when deformed plastically is important to avoid failures. In this research, samples were taken from a region free of solder and plastically deformed from 0 to 2.5% in a tensile machine. The samples were analyzed by chemical and electrochemical tests in NACE 177-A solution. It was concluded that the corrosion resistance was not affected by the different conditions of plastic deformation.

© 2018 Brazilian Metallurgical, Materials and Mining Association. Published by Elsevier Editora Ltda. This is an open access article under the CC BY-NC-ND license (<http://creativecommons.org/licenses/by-nc-nd/4.0/>).

## 1. Introduction

The API 5L X65 steel is classified as a high resistance and low alloy steel, which presents low carbon content, less than 0.30%, good tenacity and weldability. Pipelines for petroleum industry applications are constructed according to the American Petroleum Institute technical specifications [1–3]. This steel is used in construction of long-distance, high-pressure transportation pipelines that need to show the best combination of strength and hardness to support high internal pressures [4].

The water used in this process contains many corrosive agents like carbon dioxide and hydrogen sulfide that represent an important factor in the internal corrosion of steel pipelines [5]. Besides that, transmission pipelines have residual stresses due to manufactured and welding process, which can alter the structure's load capacity when subjected to external stresses. This is a big problem, because pipelines are subject to plastic deformation by outside forces as ground liquefaction, mechanical damages and buckling [6,7]. The corrosion is responsible for half of pipelines failures, which can cause catastrophic and environmental damages [8]. In this research, samples of API 5L X65 were plastic deformed in

<sup>☆</sup> Paper was part of technical contributions presented in the events part of the ABM Week 2017, October 2nd to 6th, 2017, São Paulo, SP, Brazil.

<sup>\*</sup> Corresponding author.

E-mail: [marianaeng@uol.com.br](mailto:marianaeng@uol.com.br) (M.C. Oliveira).

<https://doi.org/10.1016/j.jmrt.2018.02.006>

2238-7854/© 2018 Brazilian Metallurgical, Materials and Mining Association. Published by Elsevier Editora Ltda. This is an open access article under the CC BY-NC-ND license (<http://creativecommons.org/licenses/by-nc-nd/4.0/>).

**Table 1 – Percentage of relative weight loss for the deformation conditions 0% and 2.5%.**

Deformation condition – sample	Mass loss for each sample	Weight loss
0% – 1	11%	10%
0% – 2	9%	
2.5% – 1	11%	10%
2.5% – 2	10%	

different percentages and corrosive tests were performed to understand how the plastic deformation can influence the corrosive behavior of the steel in an acid solution.

## 2. Methods

Samples were cut of a weld-free region of a tube and machined in a lathe. A traction machine was used to plastically deform them in 0.5%, 1.0%, 1.5%, 2.0% and 2.5%. The immersion tests were carried out according to ASTM standards G31-72 and G1-90 [9,10] for the deformation conditions of 0.0% and 2.5%. All faces of the samples were polished with emery paper. The NACE 177-A solution [11] was composed of 236.25 g of deionized H<sub>2</sub>O, 1.25 g of CH<sub>3</sub>COOH and 12.5 g of NaCl and pH 2.68. The tests were carried out in duplicate, at room temperature for 96 h. After the tests the samples were washed with

distilled water, dried and weighed. The pickling process was done with the Clark solution, which contains 50.0 g of SnCl<sub>2</sub> and 20.0 g of Sb<sub>2</sub>O<sub>3</sub> in 1.0 L of HCl 50% (v/v) at room temperature.

Each immersion cycle was 1 min and the pickling finished when the difference between two successive weights differed by 0.0001 g [12]. The preparation of the working electrodes for the electrochemical tests consisted of the mechanical polishing of samples (25 mm × 25 mm × 5 mm) with emery paper (120–2500). Then, the samples were rinsed in an ultrasonic bath containing propan-2-ol and then for each deformation condition 5 replicates were made. It was used an electrochemical cell (Princeton Applied Research – PAR), an Ag/AgCl reference electrode, a Pt wire as a counter electrode, and a solution containing 236.25 g deionized H<sub>2</sub>O, 12.5 g NaCl and 1.25 g of CH<sub>3</sub>COOH (NACE 177-A) as electrolyte. The medium was depleted of oxygen, bubbling N<sub>2</sub> for 30 min before starting the experiment and also during the experiment. An Autolab potentiostat/galvanostat, model PGSTAT 302N and Nova 1.8 software was used to obtain and analyze the data. The open circuit potential (OCP) was measured for 3 h in order to verify the stability of the potential in open circuit. In order to obtain Tafel curves, the scanning was started of –250 mV to +250 mV from OCP, at 0.166 mV s<sup>-1</sup>. The impedance measurements (EIS) were performed at the OCP, applying a sinusoidal signal of 0.01 V rms, in the frequency range of 100 kHz to 10 mHz.

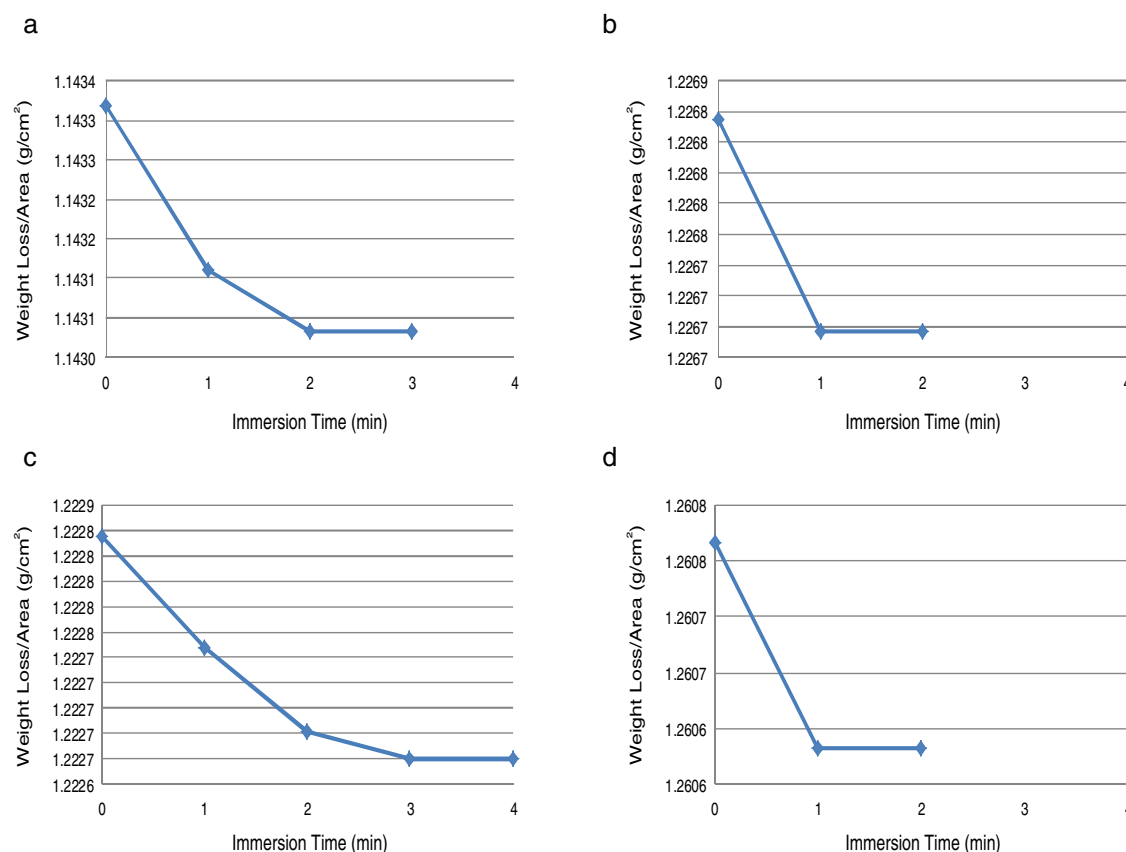


**Fig. 1 – Weight loss per area for each immersion cycle of the pickling process, plastic deformation and samples: (a) 0% – 1; (b) 0% – 2; (c) 2.5% – 1; (d) 2.5% – 2.**

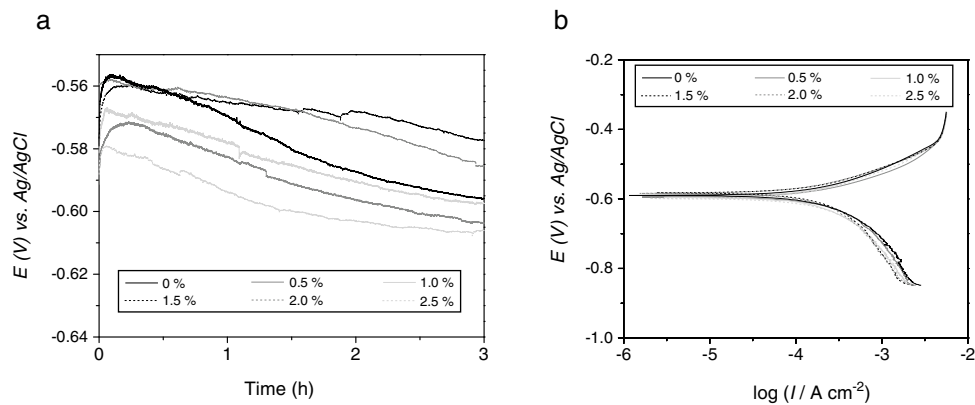


**Fig. 2 – OCP (a) and Tafel (b) curves obtained for API 5L X65 steel under different conditions of plastic deformation in a standardized acid medium (NACE 177-A).**

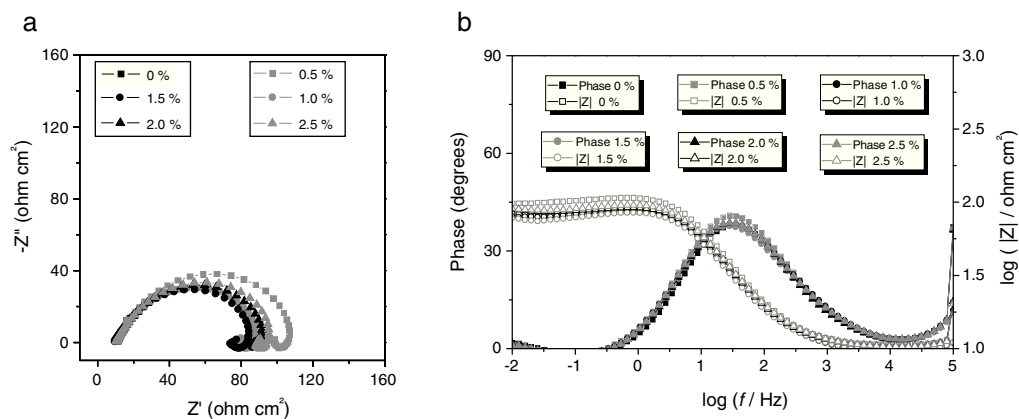


**Fig. 3 – EIS spectra of API 5L X65 steel under different conditions of plastic deformation in a standardized acid medium (NACE 177-A): Nyquist (a) and Bode (b) formats.**

### 3. Results

The pickling process was done as described in section 2 and the mass loss per area for each sample in a function of time are shown in Fig. 1.

Table 1 shows the relative weight loss for each deformation condition, which was calculated using the following equation.

$$\text{Relative weight loss} = \frac{M_i - M_f}{M_i \times A} \times 100\% \quad (1)$$

where  $M_i$  is the mass before starting the immersion test (g);  $M_f$  is the mass at the end of the pickling process (g);  $A$  is the exposed area of c-d-p (cm<sup>2</sup>).

Fig. 2 shows one of the five replicates obtained from the OCP, Fig. 2(a), and Tafel curves, Fig. 2(b), for each plastic deformation condition, where it is found that the different deformation conditions apparently do not affect the corrosion potential and the current density.

From the impedance measurements, the spectra were obtained in Nyquist format, Fig. 3(a), showing a capacitive arc at high frequencies and inductive at low frequencies. And in

the Bode format, Fig. 3(b), with only one maximum for the variation of the phase angle with the frequency suggesting an active dissolution behavior of the electrode.

The circuit proposed by Poorqasemi and collaborators [13], Fig. 4, was used to analyze the impedance curves, which fitted very well to the experimental EIS spectra obtained, Fig. 5.

### 4. Discussion

The weight loss during the pickling process presented in Table 1 show small variation,  $\leq 0.3$  g. Fig. 1 shows the graph of weight loss as a function of area, from which it can be observed that for all conditions, mass loss is minimal, which was already expected, since the material does not form a passivation film.

The graphs show the behavior required by the G1-90 standard. The resulting percentages of weight loss per unit area are equal for the two deformation conditions tested, Table 1, indicating that the percentage of plastic deformation was not sufficient to cause differences in the corrosion rate of the material when exposed to long periods. The open circuit potential, Fig. 2(a), minimally varies over time and

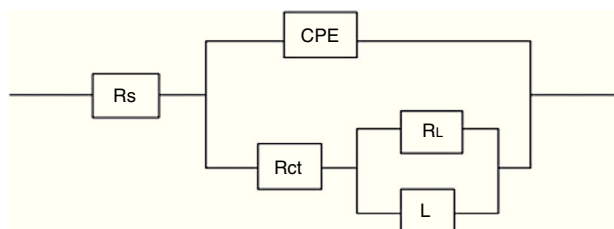


**Fig. 4 – Equivalent electrical circuit used for fitting EIS spectra.**

stabilizes at very close values on all deformation conditions. This behavior indicates that it is not a significant change in anode and cathode regions during corrosion. Fig. 2(b) presents the polarization curves, from which it can be observed that all the deformation conditions show similar profiles and corrosion rates. It is found that the polarization is controlled by activation process because there is a continuous increase of the anodic and cathodic current as the potential increases [14].

In this way, there is no formation of a passivation film due to the dissolution of the corrosion products, maintaining an exposed area always active, according to Veloz and González [15]. The EIS spectra in Nyquist format, Fig. 3(a), show a capacitive behavior at high frequencies and inductive semicircle at low frequencies, which can be explained by a process of adsorption and desorption of species at the electrode surface, such as  $\text{Cl}^-$ ,  $\text{H}^+$  [13,15]. It can be observed in Fig. 3(b) the Bode

formats showing only one maximum significantly lower than  $90^\circ$  for the phase angle stating that it is an active corrosion process.

It was used the equivalent electric circuit, Fig. 4, was used to analyze the EIS spectra, where the resistance  $R_s$  refers to the resistance of the solution, the capacitor (CPE) in parallel with the charge transfer resistance ( $R_{ct}$ ) represent the capacitive arc that can be attributed to the charge transfer reaction. The inductor (L) and its resistance ( $R_L$ ) represent the inductive arc that appears at low frequencies, and can be justified by the adsorption of electroactive species. It was obtained good agreement between calculated and experimental results, Fig. 5. In addition, comparing the values of impedance modules, at the frequency limit that tends to zero,  $|Z|_{f \rightarrow 0}$ ,  $R_p$  (Tafel) and  $R_{ct}$  (equivalent circuit modeling) are found to be all of the same magnitude, approximately  $10^2 \Omega \text{ cm}^2$ , a very low value that describes a corrosive metal surface.

## 5. Conclusions

In this work the effect of the plastic deformation on the corrosive behavior of API 5L X65 steel in acidic medium containing chloride was investigated. The tests of chemical and electrochemical corrosion indicated that the plastic deformation did not significantly affect the corrosion resistance of the steel and that the corrosion process is represented by dissolution active. A good fitting was obtained to the EIS spectra by the proposition of an equivalent electric circuit.

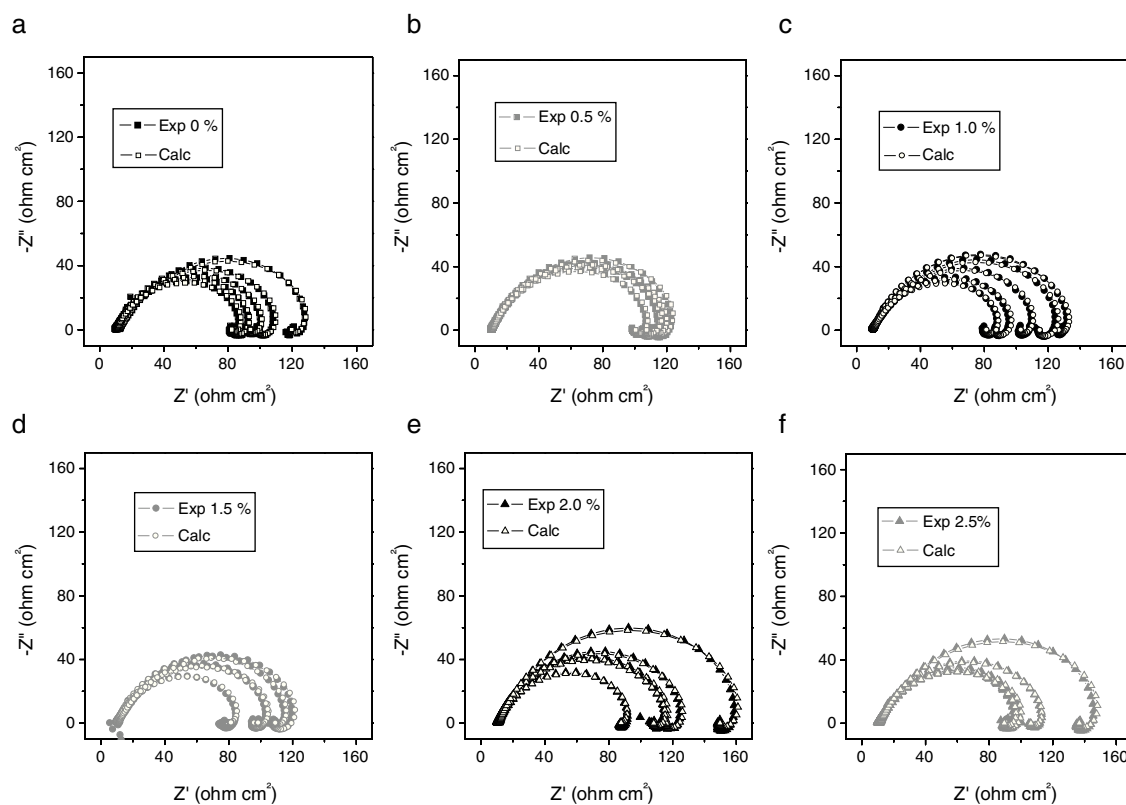


**Fig. 5 – Nyquist spectra of API 5L X65 steel at different conditions of plastic deformation.**

---

## Conflicts of interest

The authors declare no conflicts of interest.

---

## Acknowledgements

Thanks to the FAPESP (process n. 2017/11361-5) and to the Capes by financial support.

---

## REFERENCES

- [1] do Monte IR. *Caracterização Microestrutural do Aço API 5L X65 Soldado por Feixe de Elétrons com Diferentes Aportes Térmicos*. USP; 2013.
- [2] Misseno C, Morilla C. *Aços de alta resistência e baixa liga em oleodutos e gasodutos*. UNISANTA – Sci Technol 2012;1:20–4.
- [3] API 5L. Specification for line pipe. Am Pet Inst 2012;5:153, <http://dx.doi.org/10.1520/G0154-12A>.
- [4] Hashemi SH. Strength-hardness statistical correlation in API X65 steel. Mater Sci Eng A 2011;528:1648–55, <http://dx.doi.org/10.1016/j.msea.2010.10.089>.
- [5] Meresht ES, Farahani TS, Neshati J. 2-Butyne-1, 4-diol as a novel corrosion inhibitor for API X65 steel pipeline in carbonate/bicarbonate solution. Corros Sci 2012;54:36–44, <http://dx.doi.org/10.1016/j.corsci.2011.08.052>.
- [6] Baek J, Kim Y, Kim C, Kim W, Seok C. Effects of pre-strain on the mechanical properties of API 5L X65 pipe. Mater Sci Eng A 2010;527:1473–9, <http://dx.doi.org/10.1016/j.msea.2009.10.017>.
- [7] Ju J, Lee J, Jang J, Kim W, Kwon D. Determination of welding residual stress distribution in API X65 pipeline using a modified magnetic Barkhausen noise method. Int J Press Vessel Pip 2003;80:641–6, [http://dx.doi.org/10.1016/S0308-0161\(03\)00131-5](http://dx.doi.org/10.1016/S0308-0161(03)00131-5).
- [8] Terzi R, Mainier FB. *Monitoramento da corrosão interna em plataformas offshore*. Tecno-Lógica 2008:14–21.
- [9] ASTM G31 72. [s.d.].
- [10] Designation:G1-90 – Standard practice for preparing, cleaning, and evaluating corrosion test specimens. vol. 90. 1999.
- [11] ANSI/NACE TM0177. *Standard test method laboratory testing of metals for resistance to sulfide stress cracking and stress corrosion cracking in H2S environments*. Houston; 2016.
- [12] de Almeida NL, Panossian Z. *Corrosão atmosférica: 17 anos*. São Paulo: IPT; 1999.
- [13] Poorqasemi E, Abootalebi O, Peikari M, Haqdar F. Investigating accuracy of the Tafel extrapolation method in HCl solutions. Corros Sci 2009;51:1043–54, <http://dx.doi.org/10.1016/j.corsci.2009.03.001>.
- [14] Tait W. *An introduction to electrochemical corrosion testing for practicing engineers and scientists*. PairODocs Publ 1994;26:138.
- [15] Veloz MA, González I. *Electrochemical study of carbon steel corrosion in buffered acetic acid solutions with chlorides and H<sub>2</sub>S*. Electrochim Acta 2002;48:135–44.